

Dense atom clouds in a holographic atom trap

R. Newell, J. Sebby, and T. G. Walker

Department of Physics, University of Wisconsin—Madison, Madison, Wisconsin 53706

Received November 14, 2002

We demonstrate the production of high-density cold ^{87}Rb samples (2×10^{14} atoms/cm³) in a simple optical lattice formed with YAG light that is diffracted from a holographic phase plate. A loading protocol is described that results in 10,000 atoms per $10 \mu\text{m} \times 10 \mu\text{m} \times 100 \mu\text{m}$ unit cell of the lattice site. Rapid free evaporation leads to a temperature of $50 \mu\text{K}$ and phase space densities of $1/150$ within 50 ms. The resulting small, high-density atomic clouds are very attractive for a number of experiments, including ultracold Rydberg atom physics. © 2003 Optical Society of America
OCIS codes: 020.7010, 020.5780.

Conventional light-force atom traps are limited in density by radiation trapping to typically 10^{11} cm^{-3} (Refs. 1 and 2); here we report densities in far-off-resonance traps³ (FORTs) that exceed this limit by 3 orders of magnitude and are comparable to Bose–Einstein condensate densities. We show that FORTs can achieve these densities in tens of milliseconds, compared with tens of seconds for magnetic traps. Such rapidly produced high-density sources are of particular interest for studying novel collision phenomena that do not require the coherence of Bose–Einstein condensates and yet can be exploited for quantum manipulation and entanglement of atoms. These sources are also attractive for evaporative cooling; two groups have recently cooled atoms to quantum degeneracy by use of FORTs.^{4,5}

FORTs use spatially varying light intensities $I(\mathbf{r})$ to produce a conservative potential $U(\mathbf{r}) = -2\pi\alpha(\lambda)I(\mathbf{r})/c$, where $\alpha(\lambda)$ is the polarizability of the atom at the FORT laser wavelength λ . At a given temperature T and number of trapped atoms N the peak density depends not directly on the trap depth but rather on its curvature: $n \sim N(\kappa/T)^{3/2}$, where $\kappa = -\partial_{\mathbf{r}}^2 U$. Therefore, one can obtain much higher densities at roughly the same trap depth by forming an interference pattern (optical lattice) to create a rapid spatial variation in the intensity. In general, for a fixed laser power and beam area, forming an interference pattern (lattice) of cell size Λ from M beams increases the trap depth over a single-beam FORT by a factor $O(M)$ and the spring constant, κ , by a factor $O(M/\Lambda^2)$. However, the number of atoms per lattice site is reduced by $O(\Lambda^3)$ so that the Λ dependence cancels and the density scales as $M^{3/2}$. Thus there is considerable freedom in choosing the geometry of lattice FORTs without sacrificing density. Our FORT exploits this freedom as described below.

For phenomena occurring at high densities ($>10^{13} \text{ cm}^{-3}$) it is desirable to construct a lattice FORT with sufficient unit cell volume that many atoms can be loaded into a given lattice site. This has been demonstrated by several groups using a variety of trap geometries: three-dimensional lattice,⁶ crossed dipole,⁴ a single retroreflected beam,^{5,7} a beam focused with an array of microlenses,⁸ and the interference of light diffracted from a holographic phase plate.⁹ In an early experiment Boiron *et al.*⁹ used a holographic phase plate and a YAG laser to construct a large Λ

Cs lattice. After applying blue Sisyphus cooling, they obtained densities of the order of 10^{13} cm^{-3} . In this Letter we use higher intensities, optimized loading, and evaporation without the aid of Sisyphus cooling to attain Rb densities exceeding 10^{14} cm^{-3} and phase space densities approaching $1/150$ after loading for only tens of milliseconds. Furthermore, our use of a multimode flash-lamp-pumped laser demonstrates the robust nature of the trap.

In our experiments we use a YAG laser to achieve an optical lattice, called a holographic atom trap (HAT), by interfering five diffracted beams from a holographic phase plate (Fig. 1). At the intersection of the five laser beams an interference pattern

$$\frac{I(\mathbf{r})}{I_0} = |\exp(ikz) + 2\beta \exp[ikz(1 - \theta^2/2)] \times (\cos kx\theta + \cos ky\theta)|^2 \quad (1)$$

is produced, and Rb atoms [$\alpha(1.06 \mu\text{m}) = 0.105 \text{ nm}^3$ (Refs. 3 and 10)] are trapped at the intensity maxima. Here $k = 2\pi/\lambda$, $\theta = 0.1 \text{ rad}$ is the diffraction angle of the four first-order beams, and $\beta^2 = 0.20$ is the intensity ratio of a first-order beam to the zeroth-order beam, I_0 . Along the \hat{z} light-propagation direction the interference fringes arise from the Talbot

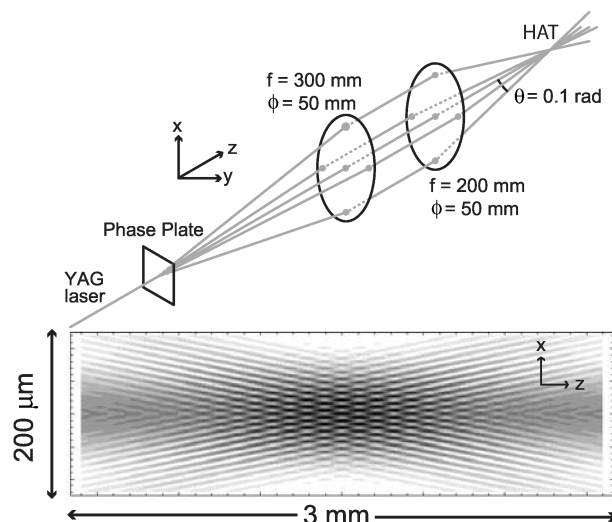


Fig. 1. Optical train used to produce the HAT and calculation of the interference pattern formed at the intersection of the five HAT beams.

effect.⁹ The resulting lattice has unit cells (microtraps) that are $10\ \mu\text{m} \times 10\ \mu\text{m} \times 100\ \mu\text{m}$ in size. With the individual beams focused to $80\ \mu\text{m}$ and a total power of 8 W, the depth of the central microtrap is $500\ \mu\text{K}$ and the oscillation frequencies are 17, 17, and $0.7\ \text{kHz}$, confirmed by parametric heating of the HAT atoms.⁷ Since the lasers are nearly copropagating, the potential is quite stable against vibrations, and the YAG laser can have a large bandwidth, in our case approximately 25 GHz. Intensity noise heating¹¹ was eliminated with an acousto-optic intensity stabilizer. The relatively large lattice sites allow many atoms ($\sim 10^4$) to be trapped in each site. The distribution of atoms in the HAT is proportional to $\exp[-U(\mathbf{r})/T]$; a calculation with $T = 50\ \mu\text{K}$ is shown in Fig. 2. As can be seen from the figure, the ratio $U(\mathbf{r})/T$ strongly favors loading atoms into the center microtraps.

This arrangement has a number of technical advantages over the crossed dipole trap geometry pioneered by Barrett *et al.* for rapid evaporation to Bose-Einstein condensates.⁴ It uses 8 W from a YAG laser and one vacuum port as opposed to 12 W from a CO_2 laser in each of two vacuum ports. Although our YAG laser is closer to resonance with the trapping transition it is still sufficiently far off resonance for Rayleigh scattering to be negligible; for the laser intensities used here, we calculate a scattering rate of 0.36 photons/s. Furthermore, using a YAG laser is advantageous in that standard materials and optical coatings work well at $1064\ \text{nm}$.

We use a probe laser propagating along the \hat{y} direction to take spatial heterodyne¹² phase images that show the atoms' isolation within the Talbot fringes and the microtraps (top of Fig. 3). Analysis gives $\sim 4 \times 10^5$ atoms per Talbot fringe, with 10% of the atoms in the central microtrap. Time-of-flight measurements indicate a temperature of $50\ \mu\text{K}$. This information and the Boltzmann distribution function given above imply peak densities exceeding $2 \times 10^{14}\ \text{cm}^{-3}$ and phase space densities of $1/150$. We observe Bragg diffraction of the probe beam from the atoms in the microtraps that appears above and below the atoms when the imaging lens is slightly defocused (bottom of Fig. 3). An interesting observation from Figs. 1 and 2 is that there should be a relative shift of the microtraps in successive Talbot fringes (Fig. 4).

The HAT's success relies on an efficient loading protocol. We begin with a vapor-cell-forced dark spot magneto-optical trap³ (MOT) with 50% of the 10^7 atoms in each of the hyperfine ground states ($5S_{1/2}F = 1, 2$) of ^{87}Rb . The dark spot is achieved by imaging of an opaque object in the hyperfine repumping beam ($F = 1 \rightarrow 5P_{3/2}F' = 2$). The trapping light ($F = 2 \rightarrow F' = 3$) is tuned three linewidths Γ below resonance and has an intensity of $72\ \text{mW}/\text{cm}^2$. We add a circularly polarized depumping laser tuned to the high-frequency side of the $F = 2 \rightarrow F' = 2$ resonance and a bias magnetic field to spin polarize the atoms in the $F = 1$ ground state. To load the HAT from the MOT, we decrease the trapping light intensity by a factor of 3, then compress the MOT by increasing the gradient magnetic field.^{14,15} These steps double the density of dark-state atoms to $4.7 \times 10^{11}\ \text{cm}^{-3}$.

After 20 ms we turn on the HAT laser. AC Stark shifts tune the repumping and trapping beams away from resonance and the depumping beam toward resonance, causing the atoms in the HAT to be extremely dark (estimated $\sim 0.1\%$ in $F = 2$).¹⁶ During the HAT loading phase we shift the trapping laser detuning to -9Γ . Time-of-flight measurements of the MOT temperature agree with the predictions of Gerz *et al.*¹⁷ throughout the loading process; in particular, we measure $15\ \mu\text{K}$ in the final high-detuning stage. The number of trapped atoms increases until it reaches steady state in $\sim 50\ \text{ms}$, then the MOT lasers are extinguished. The MOT to HAT transfer efficiency is as high as 15%.

We show in Fig. 5 the temperature and number of atoms versus time after the loading ceases. The temperature rapidly decreases to $\sim 50\ \mu\text{K}$, approximately 1/10 of the trap depth, as expected for free evaporation of atoms from the HAT.¹⁸ The evaporation is rapid

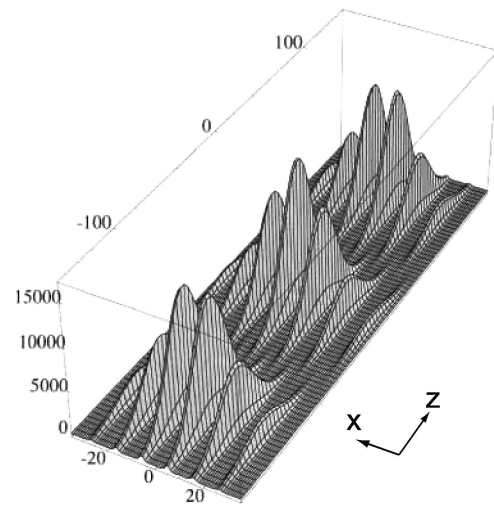


Fig. 2. Calculated density distribution of atoms in the HAT, assuming a Boltzmann distribution with a temperature equal to 1/10 the maximum trap depth. Distances are in micrometers; densities, in arbitrary units.

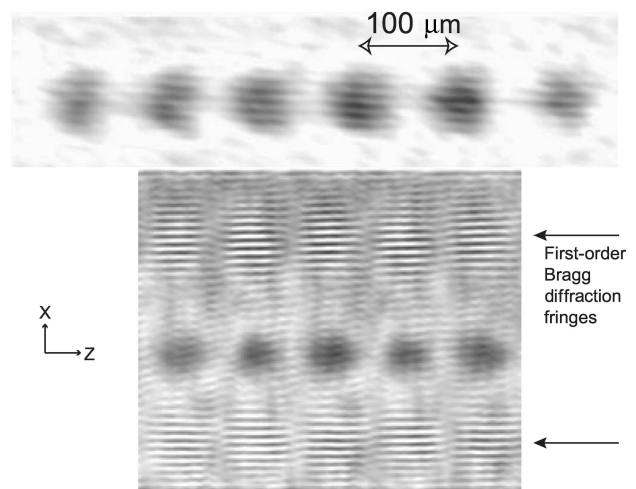


Fig. 3. Top, image showing microtraps. Bottom, first-order Bragg diffraction can be separated from the Talbot fringes by defocusing the imaging lens.

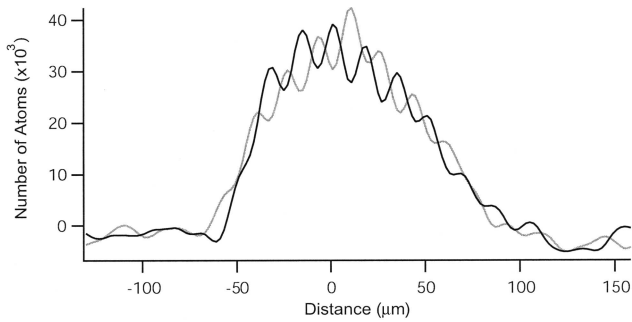


Fig. 4. Spatial profiles of two neighboring Talbot images. The microtrap structure is shifted between the two, as expected. The microtraps are not fully resolved by the imaging system.

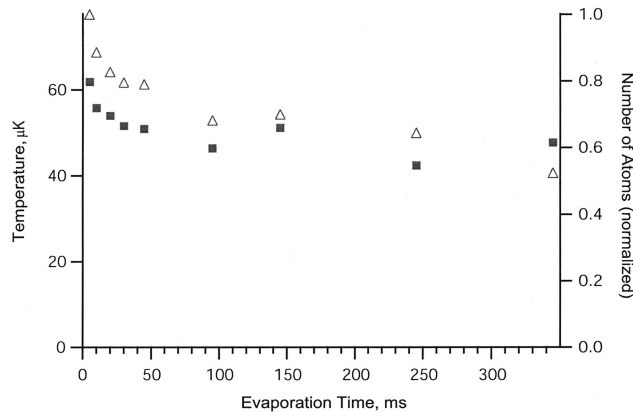


Fig. 5. Evaporative cooling of the atoms occurs after the cooling lasers are switched off. The number of atoms in a single Talbot fringe (triangles) and the temperature (squares) rapidly decrease until the temperature reaches roughly 1/10 the trap depth.

because of the very high densities; we estimate the elastic collision rate to exceed $10^4/\text{s}$. Such high collision rates make evaporative cooling very promising for the HAT, and such experiments are underway in our laboratory. Trap lifetime studies show that after the evaporation ceases the temperature stays fixed but the atoms are slowly ejected from the trap¹⁹ by background gas collisions with a time constant of ~ 500 ms, four times shorter than the MOT lifetime.

These high-density samples are of interest for a variety of experiments. In addition to obvious examples such as evaporative cooling and cold collisions, many groups are interested in ultracold Rydberg atoms. Excitation of Rydberg states with a principal quantum number of ~ 100 in our HAT will give rise to strong, long-range dipole-dipole interactions. Because atoms in our microtraps are localized within a $15\text{-}\mu\text{m}$ region, these interaction energies are >1 MHz for atoms on opposite sides of a microtrap. Consequently, excitation by a narrowband laser of more than one Rydberg atom at a time per microtrap should be greatly suppressed. This “dipole blockade” is of great interest for applications in quantum information processing²⁰ and single-atom and photon sources.²¹ Similarly, the densities are high enough to expect efficient excitation of novel long-range Rydberg molecules such as those recently proposed.^{22,23} In addition, it will be interesting

to see how the very much higher densities achieved in the HAT than with MOTs affect the production of cold plasmas.²⁴

The authors are grateful for the support of NASA, the National Science Foundation and the Army Research Office. We thank S. Kadlecik and J. Day for pivotal contributions to the imaging system and D. Steele and N. Harrison for work on early stages of the experiment. R. Newell’s e-mail address is rtnewell@wisc.edu.

References

1. T. Walker, D. Sesko, and C. Wieman, *Phys. Rev. Lett.* **64**, 408 (1990).
2. W. Ketterle, K. Davis, M. A. Joffe, A. Martin, and D. E. Pritchard, *Phys. Rev. Lett.* **70**, 2253 (1993).
3. J. D. Miller, R. A. Cline, and D. J. Heinzen, *Phys. Rev. A* **47**, R4567 (1993).
4. M. D. Barrett, J. A. Sauer, and M. S. Chapman, *Phys. Rev. Lett.* **87**, 010404 (2001).
5. S. R. Granade, M. E. Gehm, K. M. O’Hara, and J. E. Thomas, *Phys. Rev. Lett.* **88**, 120405 (2002).
6. D. J. Han, S. Wolf, S. Oliver, C. McCormick, M. T. DePue, and D. S. Weiss, *Phys. Rev. Lett.* **85**, 724 (2000).
7. S. Friebe, R. Scheunemann, J. Walz, T. W. Hänsch, and M. Weitz, *Appl. Phys. B* **67**, 699 (1998).
8. R. Dumke, M. Volk, T. Mütter, F. B. J. Buchkremer, G. Birkl, and W. Ertmer, *Phys. Rev. Lett.* **89**, 097903 (2002).
9. D. Boiron, A. Michaud, J. M. Fournier, L. Simard, M. Sprenger, G. Grynberg, and C. Salomon, *Phys. Rev. A* **57**, R4106 (1998).
10. M. A. Kadar-Kallen and K. D. Bonin, *Phys. Rev. Lett.* **68**, 2015 (1992).
11. M. E. Gehm, K. M. O’Hara, T. A. Savard, and J. E. Thomas, *Phys. Rev. A* **58**, 3914 (1998).
12. S. Kadlecik, J. Sebby, R. Newell, and T. G. Walker, *Opt. Lett.* **26**, 137 (2001).
13. M. H. Anderson, W. Petrich, J. R. Ensher, and E. A. Cornell, *Phys. Rev. A* **50**, R3597 (1994).
14. M. H. Anderson, J. R. Ensher, M. R. Matthews, C. E. Wieman, and E. A. Cornell, *Science* **269**, 198 (1995).
15. W. Petrich, M. H. Anderson, J. R. Ensher, and E. A. Cornell, *J. Opt. Soc. Am. B* **11**, 1332 (1994).
16. S. J. M. Kuppens, K. L. Corwin, K. W. Miller, T. E. Chupp, and C. E. Wieman, *Phys. Rev. A* **62**, 013406 (2000).
17. C. Gerz, T. W. Hodapp, P. Jenssen, K. M. Jones, W. D. Phillips, C. I. Westbrook, and K. Mølmer, *Europhys. Lett.* **21**, 661 (1993).
18. K. M. O’Hara, M. E. Gehm, S. R. Granade, and J. E. Thomas, *Phys. Rev. A* **64**, 051403 (2001).
19. S. Bali, K. M. O’Hara, M. E. Gehm, S. R. Granade, and J. F. Thomas, *Phys. Rev. A* **60**, R29 (1999).
20. M. D. Lukin, M. Fleischhauer, R. Cote, L. M. Duan, D. Jaksch, J. I. Cirac, and P. Zoller, *Phys. Rev. Lett.* **87**, 037901 (2001).
21. M. Saffman and T. G. Walker, *Phys. Rev. A* **66**, 065403 (2002).
22. C. H. Greene, A. S. Dickinson, and H. R. Sadeghpour, *Phys. Rev. Lett.* **85**, 2458 (2000).
23. C. Boisseau, I. Simbotin, and R. Cote, *Phys. Rev. Lett.* **88**, 133004 (2002).
24. T. C. Killian, M. J. Lim, S. Kulin, R. Dumke, S. D. Bergeson, and S. L. Rolston, *Phys. Rev. Lett.* **86**, 3759 (2001).